Contents list available at CBIORE journal website

International Journal of Renewable Energy Development

Journal homepage: https://ijred.cbiore.id

Research Article

Impact of crosslinking on quaternary ammonium poly(vinyl alcohol)/polyquaternium-7 anion exchange membranes for alkaline polymer electrolyte fuel cells

Asep Muhamad Samsudin[a,b*], Nur Rokhati[a,b], Nor Basid Adiwibawa Prasetya[c], Andri Cahyo Kumoro[a], Didi Dwi Anggoro[a], Kharissa Nasher[a], Dhiky Wahyudi[a], Michaela Roschger[d], Viktor Hacker[d]

[a]*Department of Chemical Engineering, Faculty of Engineering, Diponegoro University, Indonesia*

[b]*Membrane Research Center, Diponegoro University, Indonesia*

[c]*Department of Chemistry, Faculty of Science and Mathematics, Diponegoro University, Indonesia*

[d]*Institute of Chemical Engineering and Environmental Technology, Graz University of Technology, Austria*

Abstract. Alkaline Polymer Electrolyte Fuel Cells (APEFCs) have emerged as a promising candidate for clean energy production. Anion exchange membrane (AEM) is an essential element of alkaline polymer electrolyte fuel cells for its role in facilitating hydroxide ion conduction. The objective of this study is to investigate the effect of a glutaraldehyde-based crosslinker solution on the performance of anion exchange membranes (AEMs) fabricated using quaternary ammonium poly (vinyl alcohol) (QPVA) as the backbone polymer and polyquaternium-7 as the second polymer. The introduction of a glutaraldehyde-based crosslinking agent was purposed to enhance membrane stability and reduce excessive swelling. The study evaluates the impact of varying glutaraldehyde concentrations on membrane performance. FTIR analysis confirms the presence of key functional groups of QPVA, polyquaternium-7, and the crosslinking agent. SEM images reveal that the membranes demonstrate dense and homogeneous physical structure. The results show that water uptake, swelling degree, ion exchange capacity (IEC), and hydroxide conductivity are influenced by the concentration of the glutaraldehyde solution. The QP-GA-13 AEM exhibited the best overall performance, achieving the highest tensile strength of 31.1 MPa and the highest hydroxide ion conductivity of 4.15 mS cm^{-1} at 70°C. In single-cell tests, this membrane delivered a maximum power density of 85 mW cm^{-2} and a current density of 350 mA cm^{-2} at 80°C under humidified oxygen conditions.

Keywords: poly (vinyl alcohol); polyquaternium-7; glutaraldehyde; fuel cell; anion exchange membranes

Received: 27th Nov 2024; Revised: 6th April 2025 ; Accepted: 8th May 2025; Available online: 20th May 2025

1. Introduction

The growing need for sustainable and clean energy sources has intensified research into renewable energy technologies. While traditional renewable energy sources, such as solar, wind, and hydropower, have garnered significant attention, they often suffer from limitations such as intermittency, high capital costs, and storage challenges (J. Zhang, 2024). These drawbacks hinder their ability to consistently meet the demand for a continuous and reliable energy supply. To overcome these issues, alternative renewable energy solutions, including fuel cells, have been explored to complement and enhance the efficiency of conventional renewable energy systems (Al-Shetwi, 2022).

Among the various fuel cell technologies, Alkaline Polymer Electrolyte Fuel Cells (APEFCs) have emerged as a promising candidate for clean energy production. Unlike the well-established proton exchange membrane fuel cells (PEMFCs), which utilize proton-conducting membranes and acidic environments, APEFCs operate in an alkaline environment and rely on anion-conducting membranes. This difference offers several advantages, including the potential to use non-precious metal catalysts like nickel or silver, which can significantly reduce costs. Furthermore, APEFCs exhibit improved oxygen reduction reaction (ORR) kinetics in alkaline media, leading to enhanced fuel cell performance and greater operational flexibility (Tao *et al.*, 2024; G. Zhao *et al.*, 2021).

One of the key components of APEFCs is the Anion Exchange Membrane (AEM), which plays a vital role in enabling ion transport within the fuel cell. AEMs consist of a polymer backbone that is functionalized with immobilized ionic groups, typically quaternary ammonium, which serve as fixed positive charges. These fixed charges are paired with mobile counter-ions, typically hydroxide (OH^-) ions in APEFCs, which migrate through the membrane during operation to facilitate electrochemical reactions. The membrane must exhibit

* Corresponding author
Email: asep.samsudin@live.undip.ac.id (A. M. Samsudin)

https://doi.org/10.61435/ijred.2025.60897
ISSN: 2252-4940/© 2025.The Author(s). Published by CBIORE

excellent ionic conductivity, chemical stability in an alkaline environment, and adequate mechanical strength to maintain fuel cell performance over time (Samsudin, Bodner, et al., 2022).

Various methods have been proposed for the preparation of AEMs, each offering distinct advantages depending on the intended application. These methods include solution casting (Samsudin, Abdullah, *et al.*, 2024), pore-filling (Son *et al.*, 2020), sol-gel techniques (Y. Wang et al., 2020), hot pressing *(Daud et al.*, 2021), radiation-induced graft polymerization (Y. Zhao *et al.*, 2020), and electrospinning (Samsudin, Roschger, *et al.*, 2022). Among these, solution casting is the most widely used due to its simplicity, scalability, and the ability to produce homogeneous membranes with well-controlled thickness (Samsudin, Bodner, *et al.*, 2022). In this technique, a polymer solution containing ion-conducting groups is cast onto a substrate and allowed to evaporate, forming a solid film. The solution casting method offers advantages such as ease of processing, cost-effectiveness, and suitability for large-scale production, making it an attractive choice for AEM fabrication (Samsudin, Bodner, *et al.*, 2022).

Many AEMs have been synthesized using quaternized polymers with aromatic backbones, such as poly(sulfone)(Mothupi & Msomi, 2023), poly(ether sulfone) (Du, Huang, *et al.*, 2022; Du, Li, *et al.*, 2022), poly(ether ether ketone) (Ayaz *et al.*, 2022), and poly(2,6-dimethyl-1,4-phenylene oxide) (Basso Peressut *et al.,* 2023). These polymers are often functionalized with ion-conducting groups, such as quaternary ammonium (Vijayakumar *et al.*, 2021), imidazolium (Jheng *et al.*, 2021), pyridinium (Ayaz *et al.*, 2023), phosponium (Liu *et al.*, 2016), or guanidinium (Xue *et al.*, 2020), introduced through chloromethylation or bromination reactions followed by quaternization with cationic species such as trimethylamine or guanidinium hydrochloride. While these AEMs exhibit excellent chemical stability and ionic conductivity, they suffer from certain disadvantages, such as high production costs, limited mechanical flexibility, and challenges in maintaining long-term stability under highly alkaline conditions (Samsudin & Hacker, 2021a).

Poly(vinyl alcohol) (PVA) has emerged as a promising alternative polymer backbone for AEMs due to its hydrophilic nature, flexibility, and ease of functionalization. PVA-based membranes offer several advantages, including good film-forming ability, biocompatibility, and chemical stability in alkaline environments. Additionally, PVA can be easily modified with quaternary ammonium groups to enhance its anion conductivity. However, PVA is prone to swelling and dissolution in aqueous environments, which can compromise its mechanical properties and ion-exchange capacity (Samsudin, Roschger, *et al.*, 2022; J. Wang *et al.*, 2024).

To address the limitations of PVA-based AEMs, crosslinking has been widely employed to improve membrane stability and performance. Crosslinking can be either thermal or chemical. Thermal crosslinking involves the application of heat to induce bond formation between polymer chains, while chemical crosslinking uses agents to create covalent bonds with the polymer's functional groups. Common chemical crosslinkers include dialdehydes (e.g., glutaraldehyde), dicarboxylic acids (e.g., citric acid, succinic acid), dianhydrides, sulfosuccinic acid, and trisodium trimetaphosphate (Sonker *et al.*, 2018). Among these methods, glutaraldehyde is frequently used due to its effectiveness in creating stable covalent bonds between polymer chains, thereby enhancing the membrane's mechanical strength and resistance to swelling (Samsudin & Hacker, 2021b).

In this study, quaternary ammonium poly(vinyl alcohol) (QPVA) was used as the backbone polymer, while polyquaternium-7, another quaternary ammonium-containing polymer, served as an additional anion-conducting component within the PVA-based AEM. Polyquaternium-7 was chosen due to its high ionic conductivity, excellent chemical stability, and biocompatibility (Samsudin, Abdullah, *et al.*, 2024). However, since QPVA lacks water stability and polyquaternium-7 is water-soluble, crosslinking was necessary to enhance membrane integrity. Glutaraldehyde was employed as a chemical crosslinker alongside thermal crosslinking to improve mechanical strength and stability. This study aims to evaluate the impact of varying glutaraldehyde concentrations on the properties and performance of QPVA/polyquaternium-7 AEMs for APEFC applications.

2. Methods

2.1 Materials

Quaternary ammonium poly(vinyl alcohol) (with a hydrolysis level of 85.5–88.0% and viscosity ranging from 18-22 mPa.s) was procured from Mitsubishi Chemical Corporation, Tokyo, Japan. Polyquaternium-7 (poly(acrylamide-co-diallyl dimethylammonium chloride), 10 wt.% in H_2O, with a viscosity of 9,000-25,000 cP) and nano-alumina (Al_2O_3, <50 nm particle size) were the products of Sigma-Aldrich. Meanwhile, glutaraldehyde (50 wt.% in H_2O) was supplied by Merck. Anion exchange ionomer solution (fumion® FAA-3, 10 wt.% in NMP) and its corresponding membrane (fumasep® FAA-3-50, 50 µm thickness), carbon cloth (0.406 mm thickness), and carbon paper (29 BC, 0.235 mm thickness) were supplied by the Fuel Cell Store. A commercial Pt/C catalyst (20% Pt on carbon black, with a surface area of 10,000 m^2/g) was obtained from Alfa Aesar. Potassium hydroxide (AR), hydrochloric acid (AR), and acetone (AR) were also purchased from Merck.

2.2 Polymers solution preparation

A 10 wt.% QPVA solution was prepared by dissolving Gohsenx™ K-434 in distilled water at 80°C, with overnight stirring to attain homogeneity. A 5 wt.% polyquaternium-7 solution was independently prepared by diluting a 10 wt.% solution from Sigma-Aldrich with distilled water. The 10 wt.% QPVA and 5 wt.% polyquaternium-7 solutions were subsequently mixed in an ambient environment for 4 hours in 1:0.5 mass ratios.

2.3 AEMs preparation

The pre-formulated QPVA/PQ7 solution was applied onto a glass substrate utilizing a casting knife featuring an aperture of 50 µm. The wet membrane film was let to dry under ambient conditions for 48 hours. Upon complete moisture evaporation, the membrane was thoroughly peeled off the glass plate and cut according to the specific requirements for each characterization. The membrane was then heated at 130°C for one hour. Following the heat treatment, the membrane was immersed in a crosslinking solution. Various concentrations of crosslinking solution were prepared by dissolving glutaraldehyde in acetone, with a small amount of hydrochloric acid as a catalyst to allow the crosslinking process. The samples were labeled as shown in Table 1. Figure 1 illustrates the experimental procedure implemented in this study, providing a step-by-step overview of

Table 1
Sample names and formulation of crosslinker solutions

AEM Samples	Glutaraldehyde (wt.%)	Acetone (wt.%)	Distilled water (wt.%)
QP-GA-2	2	94	4
QP-GA-5	5	85	10
QP-GA-8	8	76	16
QP-GA-10	10	70	20
QP-GA-13	13	61	26

the methods applied, which began from membrane preparation and crosslinking to characterization and performance evaluations.

2.3 Structural Characterization

The structural properties of the membranes were investigated using a Spectrum Two IR spectrometer (Perkin-Elmer). Fourier Transform Infrared (FTIR) spectroscopy was utilized to analyze the key functional groups and verify the occurrence of crosslinking within the membranes. The FTIR spectra were collected in the range of 4000–400 cm^{-1}, and the resulting data were analyzed to observe characteristic peaks corresponding to the polymer backbone and crosslinking agents.

2.4 Morphological Characterization

The surface morphology of the membranes was examined using Scanning Electron Microscopy (SEM) on a JEOL JSM-6510LA instrument operated at an accelerating voltage of 10 kV. The membranes were coated with a thin conductive layer via sputtering prior to imaging. SEM images were captured to observe the microstructure and surface morphology of the membranes, providing insights into their structural features and uniformity

2.5 Mechanical Properties

The mechanical properties of AEMs, represented by tensile strength, were assessed using a universal testing machine. Membranes were cut into strips with a length of 30 mm, and the tests were performed at a constant speed of 1 mm/s. These tensile tests were essential for evaluating the strength and flexibility of the membranes, providing key insights into their durability and mechanical robustness under standard operating conditions.

2.6 Thermal Stability

Thermogravimetric analysis (TGA) was conducted to evaluate the thermal stability of the membranes using a STA 449 C apparatus (Netsch). This technique measures changes in the sample's weight as a function of temperature to determine the thermal decomposition temperature and the stability of the membranes. The membrane samples were heated from ambient temperature to 600°C at a controlled heating rate of 10°C per minute under a nitrogen atmosphere to ensure an inert environment and prevent oxidative degradation.

2.7 Ion Exchange Capacity (IEC)

The ion exchange capacity of the AEMs was evaluated using the back titration method. IEC was used to quantify the membranes' ability to exchange hydroxide ions, a key property for assessing their electrochemical performance. In this measurement, AEM samples were first immersed in 1 M KOH solution for 24 hours to fully exchange the Cl^- ions with OH^- ions. Afterward, the membranes were thoroughly rinsed with distilled water for 24 hours. This washing process was performed to remove any residual KOH that might remain in or on the membrane and potentially interfere with the subsequent titration. After rinsing, the membranes were immersed in 0.01 M HCl solution, where the hydroxide ions in the membrane were neutralized by the acid. The remaining HCl in the solution, which had not reacted with the membrane, was quantified by titration using 0.01 M NaOH. The volume of NaOH required to neutralize the unreacted HCl was carefully recorded. The IEC was calculated based on the amount of titrant used, which corresponds to the membrane's capacity to exchange hydroxide ions. The IEC is calculated using the formula (1):

$$\mathbf{IEC} = \frac{(\mathbf{V_a}-\mathbf{V_b})\boldsymbol{C}_{\mathbf{NaOH}}}{\mathbf{W_{dry}}} \quad (1)$$

where V_a is the initial volume of 0.01 M HCl solution added (in mL), V_b is the volume of 0.01 M NaOH titrant needed to

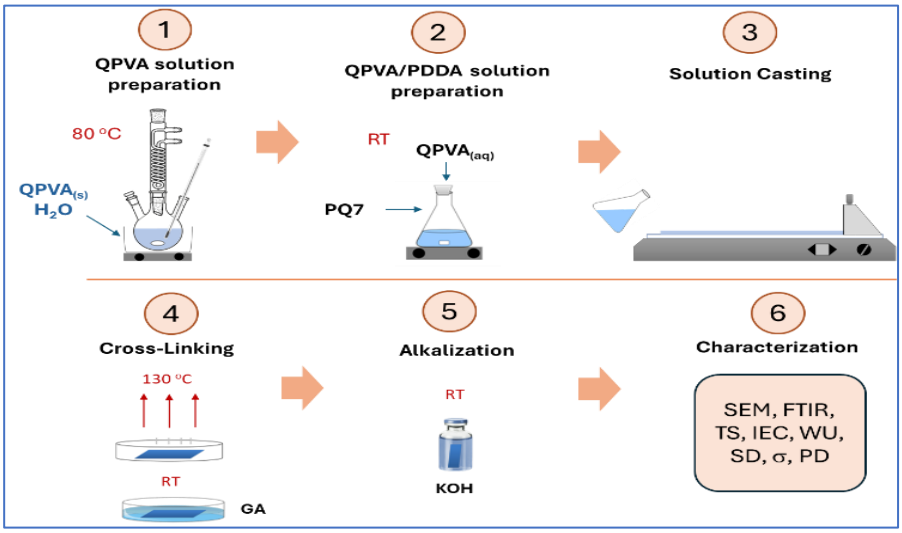

Fig. 1 Scheme of Experimental Procedure

neutralize the remaining HCl after the experiment (in mL), C_{NaOH} is the concentration of the NaOH solution (0.01 M), and W_{dry} is the dry weight of the membrane (in mg).

2.8 Water Uptake

The water uptake (WU) of the AEMs was assessed to evaluate their ability to absorb and retain water. This was done by immersing dry membranes in distilled water for 24 hours at ambient conditions to ensure thorough hydration. The membranes were weighed prior to and after immersion to determine the amount of water absorbed. The WU was then calculated using Equation 2, providing a quantitative measure of the hydration capacity of the membranes.

$$\mathbf{WU} = \frac{\mathbf{W_{wet} - W_{dry}}}{\mathbf{W_{dry}}} \mathbf{x\ 100\%} \quad (2)$$

where W_{wet} and W_{dry} represent the weight of the wet and dry membranes, respectively.

2.9 Swelling Degree

The swelling degree of the membranes was determined by immersing the membranes in distilled water for 24 hours. The volume of the membranes was measured before and after immersion, and the swelling degree was calculated using the formula (3):

$$\mathbf{WU} = \frac{\mathbf{V_{wet} - V_{dry}}}{\mathbf{V_{dry}}} \mathbf{x\ 100\%} \quad (3)$$

where V_{wet} and V_{dry} represent the volume of the wet and dry membranes, respectively.

2.10 OH^- Conductivity

The hydroxide ion conductivity of AEMs was determined using Electrochemical Impedance Spectroscopy (EIS). In this measurement, a four-electrode conductivity clamp (Bekktech BT110 LLC, Scribner Associates, USA) was used. The clamp was paired with a Gamry Reference 600 potentiostat for the measurements. The impedance data were collected across a frequency range of 0.1 Hz to 10 kHz using an alternating current (AC) potential of 50 mV. The OH^- conductivity was calculated using the corresponding equation 4:

$$\boldsymbol{\sigma} = \frac{\mathbf{L}}{\mathbf{R.A}} \quad (4)$$

where σ represents the conductivity (mS cm^{-1}), L is the thickness of the membrane (cm), R denotes the membrane resistance (Ω), and A is the cross-sectional area of the membrane (cm^2) in contact with the electrodes.

2.11 Single-cell Performance Test

The performance of the QP-GA AEM was evaluated using a custom-built alkaline direct ethanol fuel cell (ADEFC). The cathode utilized an Ag−MnxOy/C catalyst, while the anode employed a PdNiBi/C catalyst, both supported on Vulcan XC72R carbon (Roschger *et al.,* 2022). The catalysts were prepared as ink by mixing with isopropanol, water, and an ionomer (Nafion ionomer), and the mixture was applied to the gas diffusion layer (GDL) via ultrasonic spray coating (Sonotek, USA). Carbon cloth was used as the GDL at the anode, while carbon paper was employed at the cathode. Optimal catalyst loadings of 0.5 mg cm^{-2} for the anode and 0.25 mg cm^{-2} for the cathode were achieved (Roschger, Wolf, Mayer, *et al*., 2023).

Before measurements, the membranes underwent pretreatment by immersion in 1 M KOH solution for 24 hours. The membrane electrode assembly (MEA) was constructed by assembling the treated membrane with the prepared GDLs and securing them within the cell. Performance measurements were carried out at various conditions, including room temperature, 60 °C, and 80 °C, with and without humidified oxygen. The cell was supplied with 5 M KOH and 3 M ethanol at a flow rate of 5 mL min^{-1} at the anode, while the cathode received either pure or humidified oxygen at a flow rate of 25 mL min^{-1}. Polarization curves were obtained using a Zahner IM6ex potentiostat combined with a PP240 power potentiostat (Zahner-Elektrik GmbH & Co. KG, Kronach-Gundelsdorf, Germany).

3. Results and Discussion

3.1 Chemical Structure

The FTIR spectra shown in Figure 2 illustrate the impact of varying glutaraldehyde (GA) concentrations on the structural characteristics of QPVA/Polyquaternium-7 membranes. The sample without crosslinker (QP non-GA) exhibits a strong, broad peak around 3300 cm^{-1}, attributed to the O–H stretching vibrations of the hydroxyl groups in poly(vinyl alcohol) (PVA). As the concentration of GA increases, the intensity of this O–H stretching peak diminishes, suggesting that more hydroxyl groups reacted with GA to form acetal linkages. This indicates a successful crosslinking reaction, as the hydroxyl groups are progressively consumed in forming covalent bonds, strengthening the polymer network.

The C–H stretching peak at 2923 cm^{-1}, characteristic of the aliphatic C–H bonds present in both PVA and Polyquaternium-7, remains relatively constant across the spectrum, with only minor changes in intensity. This consistency suggests that the crosslinking process primarily targets the hydroxyl groups without significantly altering the aliphatic backbone of the polymers. This stability of the C–H stretching region further supports the fact that the main effect of crosslinking is on the functional groups rather than the polymer backbone, thereby preserving the membrane's mechanical integrity.

A decrease in the intensity of the C=O stretching peak at 1728 cm^{-1} is observed with higher GA concentrations. This

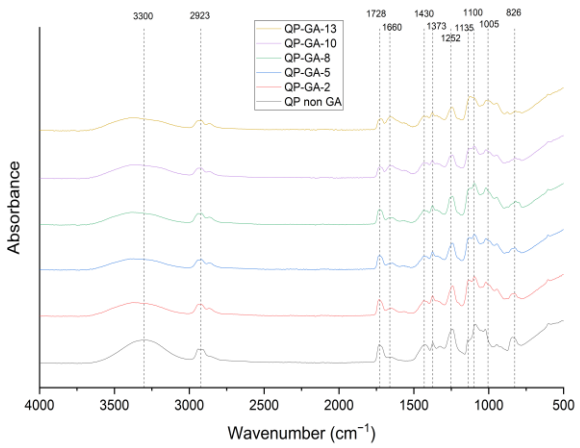

Fig. 2 IR Spectra of AEMs with different concentrations of GA as crosslinker

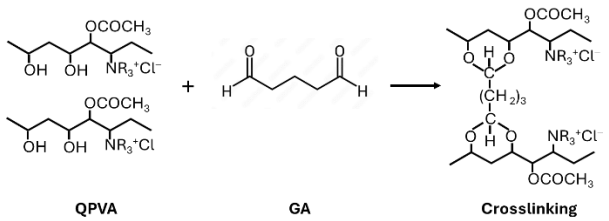

Fig. 3 Crosslinking reaction between QPVA and GA

reduction suggests that the carbonyl groups of glutaraldehyde are increasingly consumed during the crosslinking reaction with the hydroxyl groups of PVA, forming acetal linkages. The diminishing carbonyl signal implies the successful formation of crosslinked networks, particularly in QP-GA-10 and QP-GA-13, which corresponds with improved membrane stability under alkaline fuel cell operating conditions.

Interestingly, the intensity of the C=N stretching band around 1660 cm^{-1}, attributed to the quaternary ammonium groups in polyquaternium-7, increases slightly with higher GA concentrations. While no additional C=N groups are formed during the crosslinking process (Samsudin, Rokhati, *et al.,* 2024; Zhou *et al*., 2020), this increase may be due to enhanced molecular orientation or polymer chain interactions within the more densely crosslinked network. This observation suggests that the ionic functional groups remain intact and are potentially better organized, preserving the membrane's anion exchange functionality.

An increase in the absorption band at 1135 cm^{-1} is observed with increasing GA concentrations. This band is attributed to the asymmetric stretching of C–O–C bonds, which is characteristic of acetal linkages formed during the crosslinking reaction between glutaraldehyde and the hydroxyl groups of PVA (Gadhave *et al*., 2019; Z. Zhang *et al*., 2020). The gradual intensification of this peak confirms the progressive formation of a crosslinked network, supporting the enhanced structural integrity of the membrane at higher crosslinker levels. Other peaks at 1373 cm^{-1}, 1100 cm^{-1}, and 826 cm^{-1}, associated with various C–H bending and C–O stretching modes, also exhibit minor shifts or increases in intensity as GA concentration increases.

The FTIR spectra in Figure 2 show that increasing the GA concentration from 0% to 13% in the QPVA/Polyquaternium-7 membranes affects the membrane's structural properties. The progressive reduction in the O–H stretching intensity and the enhancement of the C=O and C–O–C stretching peaks confirm that higher GA concentrations lead to more extensive crosslinking, creating a stronger, more durable network. Importantly, the quaternary ammonium groups responsible for ionic conductivity remain intact throughout the crosslinking process, preserving the membrane's functionality.

3.2 Morphology

Figure 4 presents the SEM image of the QP-GA-13 Anion Exchange Membrane (AEM) at a magnification scale of 10 µm. The microstructure of the membrane appears homogeneous, with a smooth and uniform surface morphology. This suggests that the crosslinking process with 10% glutaraldehyde has been effective in developing a well-structured membrane without significant surface defects, cracks, or phase separations. The absence of visible pores or irregularities implies that the membrane possesses good mechanical integrity, which is crucial for maintaining its stability during fuel cell operation.

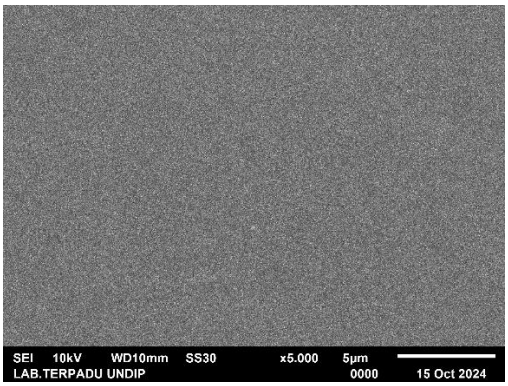

Fig. 4 SEM images of QP-GA-13 AEM (10 kV, ×5000, scale bar = 5 µm).

The uniform morphology is also indicative of a successful blending of the quaternized poly(vinyl alcohol) and polyquaternium-7, with the crosslinking process likely to help stabilize the membrane structure. The smoothness observed in the SEM image suggests that there is minimal phase segregation between the polymer components, which is advantageous for ensuring consistent ion transport across the membrane. This homogeneity plays a critical role in the membrane's performance by allowing for an even distribution of ion-conducting pathways, which can contribute to enhanced ionic conductivity and durability in alkaline polymer electrolyte fuel cells (APEFCs).

Overall, the SEM image of the QP-GA-13 membrane highlights the successful fabrication and crosslinking of the material, resulting in a membrane with a smooth, defect-free surface that is well-suited for application in fuel cells.

3.3 Thermal Stability

The thermogravimetric analysis (TGA) of the QP-GA-13 Anion Exchange Membrane (AEM) provides insights into its thermal stability and decomposition behavior, as shown in Figure 5. The TGA curve shows the weight loss of the membrane as a function of temperature, indicating distinct stages of thermal degradation.

The initial weight loss (I) observed below 100°C corresponds to the evaporation of adsorbed water and moisture within the membrane (Chen *et al*., 2022; Hdidar *et al*., 2025). This stage is typical in hydrophilic membranes like PVA-based AEMs, which

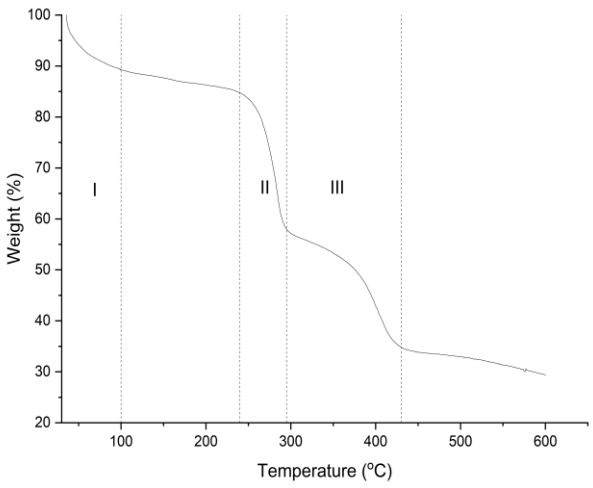

Fig. 5 TGA Results of QP-GA-13 AEM

readily absorb water. The gradual weight loss suggests that the membrane retains some water, which is characteristic of crosslinked hydrophilic materials.

The next significant weight loss (II) occurs between 240°C and 295°C. This stage represents the decomposition of the quaternary ammonium functional groups in polyquaternium-7 and the partial degradation of the PVA polymer backbone (Zhou *et al.*, 2013). The substantial drop in weight during this range indicates the breaking of chemical bonds associated with these functional groups, which is crucial for the membrane's ion exchange properties. Crosslinking with glutaraldehyde may slightly shift this degradation temperature compared to non-crosslinked membranes due to the increased stability provided by the acetal linkages.

A next major degradation step (III) occurs between 295°C and 430°C, corresponding to the thermal decomposition of the main polymer backbone, including poly(vinyl alcohol) and the remaining crosslinked network (Yang *et al.,* 2021). The sharp decrease in weight during this stage indicates the breakdown of the membrane's structural integrity. This stage marks the point at which the membrane loses most of its mechanical and chemical functionality, and it is typical for PVA-based materials.

Finally, the membrane retains approximately 30% of its original weight even at temperatures approaching 600°C, which is likely due to the formation of stable char residues. The presence of these residues suggests that the crosslinking process introduces additional stability, likely contributing to the membrane's overall durability under elevated temperatures. This residual weight could also be attributed to inorganic fillers or additives, such as nano-alumina, that do not decompose under the TGA conditions.

The TGA results demonstrate that the QP-GA membrane exhibits good thermal stability up to 200°C, with primary degradation occurring between 240°C and 430°C (Alhulaybi & Dubdub, 2024). Crosslinking with glutaraldehyde appears to enhance the thermal resistance of the membrane, making it suitable for use in applications where moderate thermal stability is required, such as in alkaline polymer electrolyte fuel cells.

3.4 Mechanical Properties

The tensile strength of QP-GA membranes, as shown in Figure 6, demonstrates the significant impact of glutaraldehyde (GA) crosslinking on the mechanical properties of the membranes. The tensile strength increases progressively with the concentration of GA, indicating improved mechanical stability as crosslinking density increases.

The non-crosslinked membrane (QP-non GA) exhibits a tensile strength of 11.2 MPa, which is the lowest among all samples. This relatively low value reflects the lack of crosslinking, leaving the polymer matrix susceptible to mechanical deformation under stress. With the introduction of 2% GA crosslinking, the tensile strength slightly improves to 12 MPa, indicating that even a small degree of crosslinking contributes to enhanced mechanical stability by forming initial acetal linkages between polymer chains.

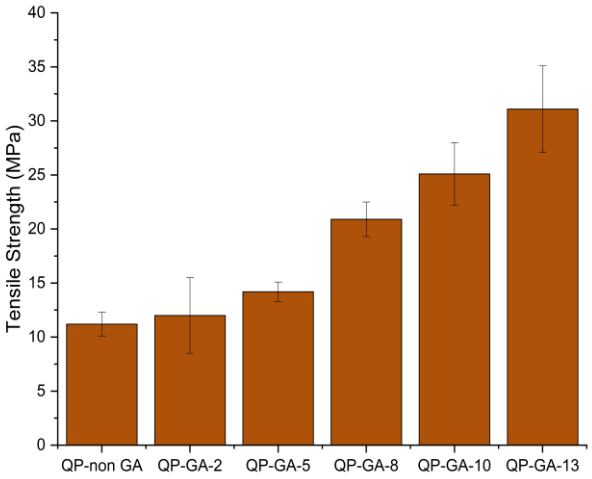

Fig. 6 Tensile Strength of QP-GA AEMs

As the GA concentration increases, the tensile strength shows a marked improvement, reaching 14.2 MPa for QP-GA-5 and 20.9 MPa for QP-GA-8. This substantial increase can be attributed to the formation of additional crosslinking bonds, which restrict polymer chain mobility and provide greater resistance to mechanical forces. The enhanced mechanical properties at these concentrations indicate that the polymer network becomes more robust and resistant to stress as the crosslinking density increases.

The QP-GA-10 and QP-GA-13 membrane exhibits the highest tensile strength values, reaching 25.1 MPa and 31.1 MPa, respectively. This significant improvement suggests that higher GA concentrations result in a dense and tightly crosslinked polymer network, offering superior mechanical strength. The QP-GA-13 membrane, with the highest GA concentration, achieves the greatest tensile strength, indicating that extensive crosslinking effectively enhances the membrane's ability to withstand mechanical deformation. A comparison of tensile strengths of various AEMs is presented in Table 2.

These results highlight the critical role of GA crosslinking in improving the mechanical properties of QP-GA membranes. The increasing tensile strength with higher GA concentrations suggests that crosslinking not only strengthens the polymer matrix but also ensures the dimensional stability of the membranes under operational conditions (Samsudin & Hacker, 2021b). This is particularly important for alkaline polymer electrolyte fuel cell (APEFC) applications, where membranes must maintain their structural integrity under mechanical and operational stresses.

Table 2
Reported tensile strength of AEMs with various backbone polymers

AEM Samples	Backbone Polymer	Tensile Stength (Mpa)	Ref.
CNSiPCS	Chitosan	11	(F. Wang *et al*., 2024)
PS-tr-QPy- 4	Polysulfone	18.1	(Ayaz *et al*., 2023)
PAEK-QP-2	Poly(arylene ether ketone)	17.3	(Ayaz *et al*., 2022)
0.30Q1.60Et0.10Pr IECNMR	Polybenzimidazoles	34.1	(Abdi *et al*., 2021)
QP-GA-13	Poly(vinyl alcohol)	31.1	This work

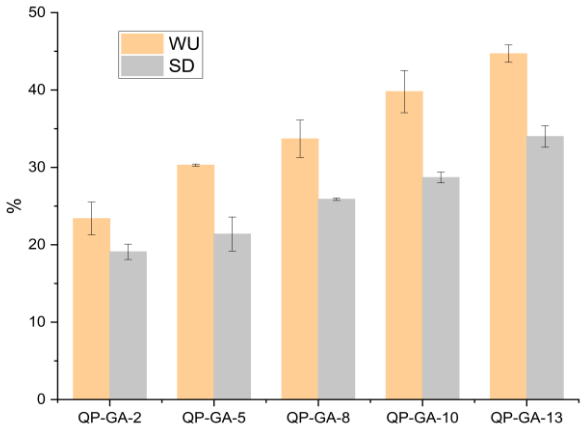

Fig. 7 Swelling Properties of QP-GA AEMs

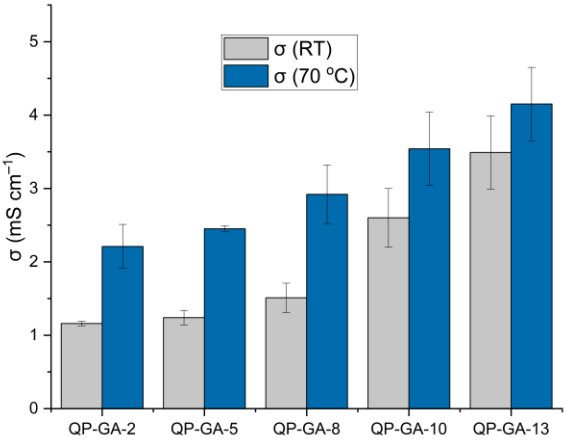

Fig. 8 Hydroxide Conductivity of QP-GA AEM at RT and 70 °C

3.4 Swelling Properties

Figure 7 shows the swelling properties of QP-GA AEMs with different glutaraldehyde (GA) concentrations, illustrating both water uptake (WU) and swelling degree (SD) as a function of crosslinking levels. As GA concentration increases from 2% to 13%, there is a notable increase in both WU and SD, confirming that higher crosslinking levels affect the membrane's capacity to absorb water and swell.

The water uptake values for the membranes increase progressively, from 23.4% in QP-GA-2 to 44.7% in QP-GA-13. This trend suggests that the higher the GA concentration, the more hydrophilic the membrane structure becomes, allowing it to absorb more water. This increase in hydrophilicity could be attributed to the presence of additional acetal linkages formed during the crosslinking process, which may introduce slightly more free volume within the membrane, facilitating water absorption. However, as the crosslinking level increases, it also limits excessive swelling, suggesting a balance between water uptake and structural stability.

Similarly, the swelling degree (SD) of the membranes shows an upward trend with increasing GA concentration, ranging from 19.1% in QP-GA-2 to 34% in QP-GA-13. This increase in SD suggests that the membranes undergo more volumetric expansion as they absorb water, which correlates with the increase in water uptake. The crosslinked structure at higher GA levels likely contributes to greater membrane integrity, preventing excessive swelling, but allows for controlled expansion. This controlled swelling is crucial in fuel cell applications, as it helps maintain membrane mechanical stability while ensuring adequate ionic pathways for hydroxide ion transport.

The observed increase in both WU and SD with higher GA concentrations implies that while the crosslinking strengthens the membrane, it still allows for sufficient hydration, which is essential for effective ionic conductivity. The QP-GA-10 and QP-GA-13 samples, which exhibit the highest values for both WU and SD, indicate an optimal balance of crosslinking, which maximizes water retention without compromising structural stability. This balance is beneficial for fuel cell operation, where membrane hydration is crucial for maintaining high ionic conductivity.

3.5 Hydroxide Conductivity

The hydroxide ion conductivity data for the QP-GA membranes at room temperature (RT) and 70°C reveal significant variations depending on the degree of crosslinking, as shown in Figure 8. At room temperature, the QP-GA-2 membrane, which is crosslinked with 2% glutaraldehyde, exhibits a conductivity of 1.16 mS cm^{-1}. This relatively low value can be attributed to the minimal crosslinking, which allows for greater ion mobility but lacks the structural stability needed to optimize ion transport. Similarly, QP-GA-5 and QP-GA-8, with conductivities of 1.24 mS cm^{-1} and 1.51 mS cm^{-1}, respectively, show that an increase in crosslinking concentration up to 8% results in only marginal improvements in conductivity at room temperature.

A pronounced conductivity enhancement is observed with the QP-GA-10 membrane, which exhibits a conductivity of 2.6 mS cm^{-1}. This suggests that a 10% glutaraldehyde concentration strikes an effective balance between structural rigidity and ion transport efficiency, leading to enhanced conductivity. The highest room-temperature conductivity, 3.49 mS cm^{-1}, is observed in the QP-GA-13 membrane, indicating that further increases in crosslinking concentration can lead to improved ion transport, likely due to the stabilization of the membrane network that prevents excessive swelling while maintaining sufficient free volume for ion mobility.

At 70°C, all membranes exhibit significantly higher conductivities, reflecting the expected increase in ion mobility at elevated temperatures. The QP-GA-2 membrane shows an increase to 2.21 mS cm^{-1}, while QP-GA-5 and QP-GA-8 display conductivities of 2.45 mS cm^{-1} and 2.92 mS cm^{-1}, respectively. These results indicate that while higher temperatures improve ion transport across all membranes (Ziv & Dekel, 2018), the effect is more pronounced for membranes with lower crosslinking concentrations, which have greater flexibility.

The QP-GA-10 membrane exhibits a conductivity of 3.54 mS cm^{-1} at 70°C, demonstrating its superior performance in balancing structural integrity with ionic conductivity. The QP-GA-13 membrane again shows the highest conductivity at 70°C, reaching 4.15 mS cm^{-1}, reinforcing the conclusion that a higher degree of crosslinking provides optimal membrane stability at elevated temperatures, which is crucial for maintaining high ion conductivity under operating conditions relevant to fuel cells.
The results demonstrate that hydroxide ion conductivity is strongly influenced by both the degree of crosslinking and the operating temperature. While lower crosslinking concentrations allow for greater flexibility and ion mobility at room temperature, higher concentrations such as in QP-GA-10 and QP-GA-13 provide the best performance at elevated temperatures due to enhanced membrane stability. These findings underscore the importance of optimizing crosslinker

content to ensure both mechanical durability and high ion conductivity in anion exchange membranes (AEMs) for fuel cell applications.

3.5 Fuel Cell Test

Figure 9 presents the polarization and power density curves for the QP-GA AEM in a single-cell alkaline polymer electrolyte fuel cell (APEFC) under various operating conditions: room temperature (RT), 60°C, and 80°C, with additional tests using humidified oxygen at 60°C and 80°C. The data show the significant impact of temperature and oxygen humidification on the fuel cell's performance, both in terms of cell potential and power density across different current densities. At room temperature, the fuel cell exhibits the lowest performance, with a sharp drop in cell potential as current density increases. The maximum current density achieved is approximately 100 mA cm^{-2}, and the peak power density is around 20 mW cm^{-2}. This is expected, as low operating temperatures reduce hydroxide ion conductivity and reaction kinetics at the electrodes, limiting both the current density and power output. When the operating temperature is increased to 60°C, the cell performance improves, reaching a maximum current density of about 180 mA cm^{-2} and a power density of approximately 40 mW cm^{-2}. Higher temperature enhances ion transport within the membrane and improves the reaction rates at the electrodes, leading to a notable improvement in both the cell potential and overall power density. However, dehydration effects at this temperature, in the absence of humidified oxygen, limit further increases in performance.

Introducing humidified oxygen at 60°C results in a substantial performance boost. The cell potential is maintained at higher values across a broader range of current densities, and the maximum current density reaches approximately 250 mA cm^{-2}. The corresponding peak power density improves to around 55 mW cm^{-2}. The use of humidified oxygen likely enhances membrane hydration, and reduces dehydration effects, thereby increasing the overall current density and power output.

The highest performance was observed at 80°C with humidified oxygen. Under these conditions, the cell reaches a maximum current density of approximately 350 mA cm^{-2} and a peak power density of around 85 mW cm^{-2}. This condition provides an optimal combination of enhanced ion conductivity and fast electrode kinetics. The humidification prevents membrane dehydration, ensuring stable ion transport and maximum utilization of reactants.

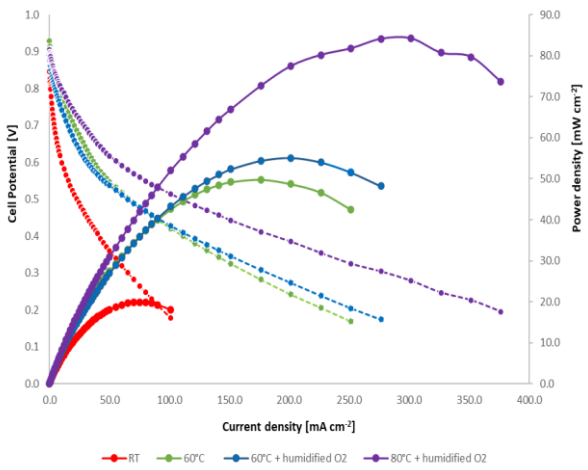

Fig. 9 QP-GA AEM Performance in APEFC

Importantly, the maximum power density achieved with the QP-GA AEM (85 mW cm^{-2} at 80°C with humidified oxygen) surpasses that of the commercial Fumasep FAA-3-50 membrane, which under the same condition achieves a maximum power density of 54.7 mW cm^{-2} (Roschger, Wolf, Billiani, *et al.*, 2023). Furthermore, the QP-GA AEM also slightly outperforms the widely studied Nafion membrane, which underwent anionic treatment, which achieves a maximum power density of 84.1 mW cm^{-2} under the same catalyst and setup conditions (Roschger, Wolf, Billiani, *et al.*, 2023). This proves that the QP-GA membrane not only exceeds the performance of a prominent commercial alkaline membrane but also competes effectively with Nafion-based membranes, which are considered benchmarks for fuel cell performance.

4. Conclusion

In this study, the performance of crosslinked quaternary ammonium poly (vinyl alcohol) (QPVA) and Polyquaternium-7 anion exchange membranes (AEMs) for alkaline polymer electrolyte fuel cells (APEFCs) was evaluated. Varying glutaraldehyde (GA) concentration for crosslinking of the membranes significantly influenced their structural, mechanical, and electrochemical properties, with the QP-GA-10 and QP-GA-13 membranes demonstrating the best performance.

The FTIR analysis confirmed successful crosslinking by the appearance of characteristic acetal linkages between the hydroxyl groups of QPVA and glutaraldehyde. The SEM images demonstrated a smooth and homogeneous membrane surface, suggesting that crosslinking improved the mechanical stability and maintained a defect-free morphology crucial for ionic conductivity. Thermogravimetric analysis (TGA) revealed that crosslinking enhanced the thermal stability of the membranes, with QP-GA-13 exhibiting the highest thermal resistance, making them suitable for high-temperature operation.

Swelling and water uptake measurements indicated that both properties increased with higher GA concentrations, with QP-GA-13 exhibiting the highest water uptake (44.7%) and swelling degree (34%). This balance between hydration and dimensional stability highlights the importance of crosslinking in ensuring effective ion transport while maintaining structural integrity. Tensile strength measurements demonstrated a consistent increase with GA concentration, with QP-GA-13 achieving the highest tensile strength (31.1 MPa), reflecting its superior mechanical stability. These findings confirm that higher crosslinking densities reinforce the membrane structure while enabling optimal hydration and swelling.

Hydroxide ion conductivity measurements showed that conductivity increased with both temperature and crosslinker concentration. At room temperature, QP-GA-13 displayed the highest conductivity (3.49 mS cm^{-1}), while the highest conductivity at 70°C was also achieved by QP-GA-13 (4.15 mS cm^{-1}). These results highlight the importance of crosslinking concentration in balancing ion transport and membrane stability.

Single-cell performance tests in APEFCs showed that fuel cell performance improved significantly with increasing temperature and oxygen humidification. The QP-GA-13 membranes displayed the highest power densities, with QP-GA-13 achieving a maximum power density of 85 mW cm^{-2} and a current density of 350 mA cm^{-2} at 80°C with humidified oxygen. These results demonstrate that high glutaraldehyde

concentrations improve the structural integrity and ionic conductivity of the membranes, leading to superior fuel cell performance.

In conclusion, the results indicate that the QP-GAmembranes, with their excellent mechanical, thermal, and electrochemical properties, are promising candidates for high-performance AEMs in APEFC applications. The combination of optimal crosslinking and operational conditions, such as elevated temperature and humidified oxygen, significantly enhances the membrane's performance, making these membranes suitable for practical fuel cell applications.

Acknowledgments

The authors sincerely thank Universitas Diponegoro for providing financial support through the Riset Publikasi Internasional Scheme under contract No. 609-99/UN7.D2/PP/VII/2024. Thanks to the World Class University Program (WCU) Universitas Diponegoro and the Indonesia Endowment Fund for Education (LPDP) for supporting the staff exchange program 2024.

Author Contributions: A.M.S..: Conceptualization, methodology, formal analysis, writing—original draft, writing—review and editing, supervision, resources, N.R.; writing—original draft, writing—review and editing, supervision, N.B.A.P..; writing—review and editing, A.C.K.: writing—review and editing, supervision, D.D.A.: writing—review and editing, supervision, M.R.: methodology, formal analysis, writing—review and editing, V.H.: writing—review and editing, supervision, All authors have read and agreed to the published version of the manuscript.

Funding: This research was funded by Universitas Diponegoro for providing financial support through the Riset Publikasi Internasional No. 609-99/UN7.D2/PP/VII/2024.

Conflicts of Interest: The authors declare no conflict of interest.

References

Abdi, Z. G., Chen, J.-C., Chiu, T.-H., Yang, H., & Yu, H.-H. (2021). Synthesis of ionic polybenzimidazoles with broad ion exchange capacity range for anion exchange membrane fuel cell application. *Journal of Polymer Science*, *59*(18), 1–13. https://doi.org/10.1002/pol.20210409

Al-Shetwi, A. Q. (2022). Sustainable development of renewable energy integrated power sector: Trends, environmental impacts, and recent challenges. *Science of the Total Environment*, *822*, 153645. https://doi.org/10.1016/j.scitotenv.2022.153645

Alhulaybi, Z. A., & Dubdub, I. (2024). Kinetics Study of PVA Polymer by Model-Free and Model-Fitting Methods Using TGA. *Polymers*, *16*(5), 1–13. https://doi.org/10.3390/polym16050629

Ayaz, S., Yao, Z. Y., Chen, Y. J., & Yu, H. Y. (2022). Preparation of poly(arylene ether ketone) based anion exchange membrane with pendant pyrimidinium and pyridazinium cation derivatives for alkaline fuel cell. *Journal of Membrane Science*, *659*(June), 120778. https://doi.org/10.1016/j.memsci.2022.120778

Ayaz, S., Yao, Z. Y., Yang, Y., & Yu, H. Y. (2023). Chemically stable anion exchange membrane with 2,6-protected pendant pyridinium cation for alkaline fuel cell. *Journal of Membrane Science*, *680*(March), 121736. https://doi.org/10.1016/j.memsci.2023.121736

Basso Peressut, A., Montagna, J., Moretti, P., Arrigoni, A., Latorrata, S., Bertarelli, C., & Dotelli, G. (2023). Development and characterization of crosslinked PPO-based anion exchange membranes for AEM fuel cells. *Solid State Ionics*, *394*(October 2022), 116212. https://doi.org/10.1016/j.ssi.2023.116212

Chen, Y., Li, P., Yuan, C., Zeng, L., Wang, J., Li, B., & Wei, Z. (2022). Anion Exchange Membranes Synthesized by Acetalization of Poly (vinyl alcohol) for Fuel Cells. *ACS Applied Energy Materials*, *5*(6), 7748–7757. https://doi.org/10.1021/acsaem.2c01217

Daud, S. N. S. S., Norddin, M. N. A. M., Jaafar, J., & Sudirman, R. (2021). Development of sulfonated poly(ether ether ketone)/polyethersulfone -crosslinked quaternary ammonium poly(ether ether ketone) bipolar membrane electrolyte via hot-press approach for hydrogen/oxygen fuel cell. *International Journal of Energy Research*, *November 2020*, 1–19. https://doi.org/10.1002/er.6453

Du, S., Huang, S., Xie, N., Zhang, T., Xu, Y., Ning, X., Chen, P., Chen, X., & An, Z. (2022). New block poly(ether sulfone) based anion exchange membranes with rigid side-chains and high-density quaternary ammonium groups for fuel cell application. *Polymer Chemistry*, *13*(30), 4395–4405. https://doi.org/10.1039/d2py00588c

Du, S., Li, S., Xie, N., Xu, Y., Weng, Q., Ning, X., Chen, P., Chen, X., & An, Z. (2022). Development of rigid side-chain poly(ether sulfone)s based anion exchange membrane with multiple annular quaternary ammonium ion groups for fuel cells. *Polymer*, *251*(April), 124919. https://doi.org/10.1016/j.polymer.2022.124919

Gadhave, R. V., Mahanwar, P. A., & Gadekar, P. T. (2019). Effect of glutaraldehyde on thermal and mechanical properties of starch and polyvinyl alcohol blends. *Designed Monomers and Polymers*, *22*(1), 164–170. https://doi.org/10.1080/15685551.2019.1678222

Hdidar, M., Chaari, M., Haddar, N., Megdiche, M., & Arous, M. (2025). Synthesis and characterization of polyvinyl alcohol crosslinked with various degrees of oxalic acid for advanced ionic conductive applications. *Ionics*, *0123456789*. https://doi.org/10.1007/s11581-025-06303-3

Jheng, L. C., Hsu, C. Y., & Yeh, H. Y. (2021). Anion exchange membranes based on imidazoline quaternized polystyrene copolymers for fuel cell applications. *Membranes*, *11*(11). https://doi.org/10.3390/membranes11110901

Liu, Y., Zhang, B., Kinsinger, C. L., Yang, Y., Seifert, S., Yan, Y., Mark Maupin, C., Liberatore, M. W., & Herring, A. M. (2016). Anion exchange membranes composed of a poly(2,6-dimethyl-1,4-phenylene oxide) random copolymer functionalized with a bulky phosphonium cation. *Journal of Membrane Science*, *506*, 50–59. https://doi.org/10.1016/j.memsci.2016.01.042

Mothupi, M. L., & Msomi, P. F. (2023). Quaternized Polyethersulfone (QPES) Membrane with Imidazole Functionalized Graphene Oxide (ImGO) for Alkaline Anion Exchange Fuel Cell Application. *Sustainability (Switzerland)*, *15*(3). https://doi.org/10.3390/su15032209

Roschger, M., Wolf, S., Billiani, A., Mayer, K., Hren, M., Gorgieva, S., Genorio, B., & Hacker, V. (2023). Study on Commercially Available Membranes for Alkaline Direct Ethanol Fuel Cells. *ACS Omega*, *8*(23), 20845–20857. https://doi.org/10.1021/acsomega.3c01564

Roschger, M., Wolf, S., Genorio, B., & Hacker, V. (2022). Effect of PdNiBi Metal Content: Cost Reduction in Alkaline Direct Ethanol Fuel Cells. *Sustainability (Switzerland)*, *14*(22). https://doi.org/10.3390/su142215485

Roschger, M., Wolf, S., Mayer, K., Billiani, A., Genorio, B., Gorgieva, S., & Hacker, V. (2023). Influence of the electrocatalyst layer thickness on alkaline DEFC performance. *Sustainable Energy and Fuels*, *7*(4), 1093–1106. https://doi.org/10.1039/d2se01729f

Samsudin, A. M., Abdullah, A., Nasher, K., & Kamal, M. T. (2024). Poly (vinyl alcohol)/Polyquaternium-7 Anion Exchange Membranes for Alkaline Polymer Electrolyte Fuel Cells. *E3S Web of Conferences*, *503*, 08006. https://doi.org/10.1051/e3sconf/202450308006

Samsudin, A. M., Bodner, M., & Hacker, V. (2022). A Brief Review of Poly (Vinyl Alcohol) -Based Anion Exchange Membranes for Alkaline Fuel Cells. *Polymer*, *14*, 3565. https://doi.org/10.3390/polym14173565

Samsudin, A. M., & Hacker, V. (2021a). Effect of Crosslinking on the Properties of QPVA/PDDA Anion Exchange Membranes for Fuel Cells Application. *Journal of The Electrochemical Society*. https://doi.org/10.1149/1945-7111/abf781

Samsudin, A. M., & Hacker, V. (2021b). Effect of Crosslinking on the Properties of QPVA/PDDA Anion Exchange Membranes for Fuel Cells Application. *Journal of The Electrochemical Society*, *168*(4), 044526. https://doi.org/10.1149/1945-7111/abf781

Samsudin, A. M., Rokhati, N., Basid, N., Prasetya, A., Nasher, K., & Kamal, M. T. (2024). Synthesis and Properties of QPVA/Polyquaternium-7 Anion Exchange Membranes for Alkaline Fuel Cells. *Journal of Membrane Science and Research*, *10*(3), 2017389 Journal. https://doi.org/10.22079/JMSR.2024.2017389.1641

Samsudin, A. M., Roschger, M., Wolf, S., & Hacker, V. (2022). Preparation and Characterization of QPVA/PDDA Electrospun Nanofiber Anion Exchange Membranes for Alkaline Fuel Cells. *Nanomaterials*, *12*(22), 3965. https://doi.org/10.3390/nano12223965

Son, T. Y., Kim, T. H., & Nam, S. Y. (2020). Crosslinked pore-filling anion exchange membrane using the cylindrical centrifugal force for anion exchange membrane fuel cell system. *Polymers*, *12*(11), 1–15. https://doi.org/10.3390/polym12112758

Sonker, A. K., Rathore, K., Nagarale, R. K., & Verma, V. (2018). Crosslinking of Polyvinyl Alcohol (PVA) and Effect of Crosslinker Shape (Aliphatic and Aromatic) Thereof. *Journal of Polymers and the Environment*, *26*(5), 1782–1794. https://doi.org/10.1007/s10924-017-1077-3

Tao, R., Shao, M., & Kim, Y. (2024). Polyarylene-Based Anion Exchange Membranes for Fuel Cells. *Chemistry - A European Journal*, *30*(41), 1–9. https://doi.org/10.1002/chem.202401208

Vijayakumar, V., Son, T. Y., Im, K. S., Chae, J. E., Kim, H. J., Kim, T. H., & Nam, S. Y. (2021). Anion Exchange Composite Membranes Composed of Quaternary Ammonium-Functionalized Poly(2,6-dimethyl-1,4-phenylene oxide) and Silica for Fuel Cell Application. *ACS Omega*, *6*(15), 10168–10179. https://doi.org/10.1021/acsomega.1c00247

Wang, F., Yang, W., Lu, H., Chen, J., Gao, S., & Shen, C. (2024). Preparation and Property Investigation of Chitosan-Based Anion- Exchange Membranes with Different Cross-Linking Structures. *Energy Fuels*, *38*(2), 1487–1495. https://doi.org/10.1021/acs.energyfuels.3c04374

Wang, J., Zhang, C., Jiang, Y., Chen, J., Gao, S., & Shen, C. (2024). Preparation and Properties of Poly(Vinyl Alcohol)-Based Anion-Exchange Membranes with Different Cross-Linked Structures. *Energy and Fuels*, *38*(13), 12087–12097. https://doi.org/10.1021/acs.energyfuels.4c01279

Wang, Y., Wang, D., Wang, J., & Wang, L. (2020). Preparation and characterization of a sol-gel derived silica/PVA-Py hybrid anion exchange membranes for alkaline fuel cell application. *Journal of Electroanalytical Chemistry*, *873*, 114342. https://doi.org/10.1016/j.jelechem.2020.114342

Xue, B., Wang, Q., Zheng, J., Li, S., & Zhang, S. (2020). Bi-guanidinium-based crosslinked anion exchange membranes : Synthesis , characterization , and properties. *Journal of Membrane Science*, *601*(February), 117923. https://doi.org/10.1016/j.memsci.2020.117923

Yang, Z., Zhang, M., Xiao, Y., Zhang, X., & Fan, M. (2021). Facile Fabrication of Poly(vinyl alcohol)/Polyquaternium-10 (PVA/PQ-10) Anion Exchange Membrane with Semi-Interpenetrating Network. *Macromolecular Materials and Engineering*, *306*(1), 1–12. https://doi.org/10.1002/mame.202000506

Zhang, J. (2024). Energy access challenge and the role of fossil fuels in meeting electricity demand: Promoting renewable energy capacity for sustainable development. *Geoscience Frontiers*, *15*(5), 101873. https://doi.org/10.1016/j.gsf.2024.101873

Zhang, Z., Liu, Y., Lin, S., & Wang, Q. (2020). Preparation and properties of glutaraldehyde crosslinked poly(vinyl alcohol) membrane with gradient structure. *Journal of Polymer Research*, *27*(8), 0–6. https://doi.org/10.1007/s10965-020-02223-0

Zhao, G., Chen, J., Sun, W., & Pan, H. (2021). Non-Platinum Group Metal Electrocatalysts toward Efficient Hydrogen Oxidation Reaction. *Advanced Functional Materials*, *31*(20), 1–12. https://doi.org/10.1002/adfm.202010633

Zhao, Y., Yoshimura, K., Mahmoud, A. M. A., Yu, H. C., Okushima, S., Hiroki, A., Kishiyama, Y., Shishitani, H., Yamaguchi, S., Tanaka, H., Noda, Y., Koizumi, S., Radulescu, A., & Maekawa, Y. (2020). A long side chain imidazolium-based graft-type anion-exchange membrane: Novel electrolyte and alkaline-durable properties and structural elucidation using SANS contrast variation. *Soft Matter*, *16*(35), 8128–8143. https://doi.org/10.1039/d0sm00947d

Zhou, T., Cai, L., & Qiao, J. (2020). Application of a novel PUB enhanced semi-interpenetrating chitosan-based anion exchange membrane. *International Journal of Energy Research*, *44*(3), 1607–1623. https://doi.org/10.1002/er.4972

Zhou, T., Zhang, J., Jingfu, J., Jiang, G., Zhang, J., & Qiao, J. (2013). Poly(ethylene glycol) plasticized poly(vinyl alcohol)/poly(acrylamide-co- diallyldimethylammonium chloride) as alkaline anion-exchange membrane for potential fuel cell applications. *Synthetic Metals*, *167*(1), 43–50. https://doi.org/10.1016/j.synthmet.2013.02.008

Ziv, N., & Dekel, D. R. (2018). A practical method for measuring the true hydroxide conductivity of anion exchange membranes. *Electrochemistry Communications*, *88*(February), 109–113. https://doi.org/10.1016/j.elecom.2018.01.021